Hysteresis and the Unobserved Congestion Branch in the Macroscopic Fundamental Diagram

Theoretical Considerations and Modeling

Yuan, Kai; Knoop, Victor L.

DOI
10.1155/2023/8797109

Publication date
2023

Document Version
Final published version

Published in
Journal of Advanced Transportation

Hindawi
Journal of Advanced Transportation
Volume 2023, Article ID 8797109, 15 pages
https://doi.org/10.1155/2023/8797109

Research Article

Hysteresis and the Unobserved Congestion Branch in the Macroscopic Fundamental Diagram: Theoretical Considerations and Modeling

Kai Yuan [1,2,3] **and Victor L. Knoop** [4]

[1]*School of Automotive and Transportation Engineering, Hefei University of Technology, Hefei 230009, China*
[2]*Engineering Research Center for Intelligent Transportation and Cooperative Vehicle-Infrastructure of Anhui Province, Hefei 230009, China*
[3]*Anhui Province Key Laboratory of Industry Safety and Emergency Technology (Hefei University of Technology), Hefei 230601, Anhui, China*
[4]*Delft University of Technology, Stevinweg 1, Delft 2628 CN, Netherlands*

Correspondence should be addressed to Kai Yuan; kyuan@hfut.edu.cn

Received 24 February 2023; Revised 13 July 2023; Accepted 24 August 2023; Published 31 August 2023

Academic Editor: Mehdi Nourinejad

The macroscopic fundamental diagram (MFD) is developed to describe traffic operations aggregated over an area. The MFD is defined by network traffic states as a relationship between the accumulation of vehicles and flow or speed of vehicles. The concept of the MFD has been applied to model traffic dynamics and to design control strategies. For various applications (e.g., routing and departure time choices), the MFD is often assumed to be of a particular shape, consisting of two branches—a free-flow branch and a congestion branch. However, empirical observations show some inconsistencies between the theoretical and the empirical MFD. First, the empirical MFD only presents free-flow branch, i.e., the congestion branch is missing. Second, the MFD presents as hysteresis loop(s). This paper explores these differences, providing insights into urban network traffic dynamics. This work takes the travelers' departure time choices and user equilibrium (UE) as starting points. We consider demand to be in UE in terms of departure time choices. Using this property of the demand profile, the paper proposes a closed-form expression for average density and outflow. Finally, we show some insights in the urban traffic dynamics: (i) an explanation of the hysteresis phenomenon solely from the perspective of departure time choices and UE and (ii) an explanation of why we hardly observe the MFD congestion branch in real life even in heavily congested networks. Our study shows that, for management purposes, the missing of congestion branch is a result of UE, rather than an indicator of congestion severity.

1. Introduction

The macroscopic fundamental diagram (MFD)—sometimes also referred to as network fundamental diagram (NFD) [1]—describes a relationship between density and average flow (or outflow) at a level of an area. There is an increasing amount of evidence for the existence of MFD relationships [2–4] from both field data and simulation studies. Figure 1 presents an empirical MFD, which is constructed using Google data.

The MFD can also be used in dynamic modeling, in the simplest case in a single-reservoir (neighborhood) framework [6]. Three key parameters for large-scale traffic flow optimization govern the shape of the MFD, that is, an aggregated network capacity, critical density, and average free-flow speed. Theoretically, the MFD consists of two branches—free-flow and congestion branch (see Figure 2). In the literature, the terms "free-flow" and "congestion" are sometimes referred to as "congestion" and "hyper-congestion," respectively.

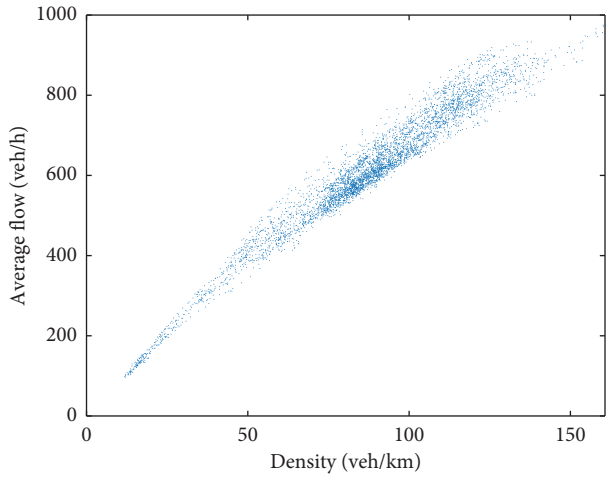

FIGURE 1: Macroscopic fundamental diagram constructed in Amsterdam using Google data. Data source can be found in [5].

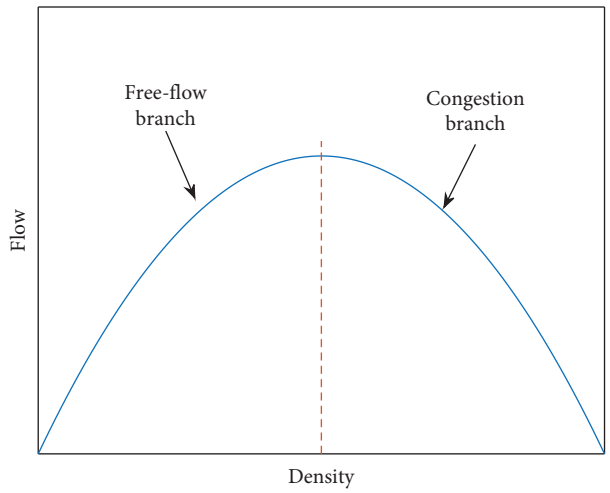

FIGURE 2: An illustration of a theoretical MFD, consisting of free-flow and congestion branches. In the literature, the "free-flow" and "congestion" are sometimes referred to as "congestion" and "hypercongestion," respectively.

The MFD shape is determined by the interplay of network structure, control, and human behavior, both in terms of driving (movement) as well as traveling (distribution). Studies using empirical data [4] and simulation data [7, 8] show that the MFD can be scattered (i.e., there is not a crisp one-to-one relation between average density and flow). A scattered MFD can also be a result of the so-called hysteresis phenomenon. As argued by Knoop et al. [8], among others, the hysteresis loop is strongly related to the spatial variance of density in a network. The heterogeneity in density over space can reduce network flow considerably. Gayah and Daganzo [9] used a two-bin model to demonstrate that clockwise hysteresis loops—in which the average flow during congestion build-up is higher than that during congestion resolution over the same density path—are less likely to occur when drivers choose their routes adaptively to avoid congestion. Daganzo et al. [10] showed that different demand loading speeds (i.e., fast and slow loading) can affect the MFD shape. Mahmassani et al. [1] showed that a higher demand level during the congestion peak could result in a larger clockwise hysteresis loop. As found by Leclercq and Paipuri [11], the MFD shape is more sensitive to the demand profile than initially expected. In this paper, we explore whether and how the MFD shape and the hysteresis phenomenon are related to departure time choices. Our hypothesis is that indeed driver adaptivity in departure time choice (i.e., drivers choosing different departure time to reduce travel delays) influences and to a degree explains both MFD shape and the hysteresis paths of network states. We will elaborate on this hypothesis further below.

The MFD has been empirically observed in several cities over the world, such as Yokohama [3], Toulouse [4], Seoul [12], Zürich [13], Shanghai [14], Lucerne [15], London [15], and Amsterdam [5]. Readers are referred to the supplementary information in [16] to see empirical MFDs in 41 cities worldwide. To the best of our knowledge, a complete MFD (showing the free-flow and the congestion branch over a full density range, see Figure 2) has only been constructed in simulations. In most cases, an empirically observed MFD only shows a free-flow branch [17]. Even when density has exceeded the critical density in some observations, the associated congestion flow does not decrease considerably compared to network capacity. Some may argue that the MFD shape (including the hysteresis phenomenon and the absence of highly congested traffic states in MFD) is a consequence of spatial heterogeneity of density [8]. Leclercq et al. [18] showed that the changes of OD matrix would result in different routing patterns in a reservoir, which could affect the shape of the MFD. Leclercq and Paipuri [11] further explained that the hysteresis pattern is a consequence of the local congestion mechanism at internal bottlenecks. The answers in the literature might describe the numerics but do not explain the (causal) mechanism behind the dynamics of this heterogeneity. In this paper, we will explore whether the departure time choices in trip scheduling decisions impact the spatial heterogeneity of density, and if so, how they do this? Clearly, the spatial variance of density is important, but a profound understanding of the mechanism behind the spatial density heterogeneity is still missing.

Except observing the MFD using empirical (or simulation) data, some studies [19–22] theoretically predicted the MFD using a method of cuts. As noted in [23, 24], the MFD constructed by cuts is a demand-independent upper envelop. The cut method could be quite useful when predicting impacts of infrastructures and control strategies on potential of traffic system. As found in [11], the cut method may not give a good approximation of the MFD that could be observed in a real network because the network loading process is dynamic. The hysteresis and the missing of congestion branch cannot be predicted and explained by the cut method.

Aghamohammadi and Laval's work [17] is one of few works that discusses possible reasons for the missing of the MFD congestion branch. As argued in [17], commuters would shift to public transportation to avoid congestion,

which will eventually prevent the network from reaching a complete gridlock. Following this line of thought, the MFD congestion branch is a result of sufficiently high demand or large delays due to congestion conditions on roads. However, this argument does not address all questions, i.e., a reason for the missing of congestion branch in almost all congested cities is still missing. In our study, we would like to propose an additional reasoning as hypothesis: the missing of the congestion branch is a property regardless of delays.

The understanding of the mechanism behind the congestion build-up is particularly relevant where MFD models are used in the context of economic appraisals, for example, in studies related to pricing. There are already papers linking the MFD to economic utility models. Some researchers present an economic model of traffic congestion that is called the bathtub model [25–33]. A review on the bathtub model can be found in [32, 34]. The model analytically derives a demand profile according to an MFD and a user equilibrium (UE) principle. The UE is also referred to as the Wardrop equilibrium [35]. The UE principle means no driver can unilaterally reduce his/her user cost by shifting to another departure time. Most of previous studies on the departure time user equilibrium are based on the bottleneck model. A comprehensive review on the bottleneck model can be found in [36]. Since the bottleneck model is too simple to represent an urban transportation network, the bathtub model is applied to address the departure time user equilibrium problem in an urban network [31, 37, 38]. The bathtub model shows that for different MFDs, there are associated demand profiles. The bathtub model is powerful because of its mathematical tractability and its inclusion of the MFD congestion branch, in contrast to, e.g., the bottleneck model [39]. But it has its limitations. For example, it does not clarify a generic principle in the match between the MFD and the demand profile, and it ignores the hysteresis. In other words, a profound understanding of the MFD shape and hysteresis loop from the perspective of departure time choices is still missing. The main objective of this paper is to reveal the generic principle, which links the demand profiles to the MFD and the hysteresis phenomenon. The generic principle will provide insights into the inconsistency between the empirical and theoretical MFD. To reach the goal, we propose an approach that, like the bathtub model, scores well in terms of mathematical tractability, conceptual simplicity, and insight, and it does this without considering any network topology.

In this paper, routing choices (for which UE may also apply) are not considered. Travelers optimize departure time choices only. Consider an area as a single reservoir with identical travelers. The demand profile, which describes vehicular flow into the reservoir along time, is a consequence of departure time choices. To model the connection between departure time choices and user costs, Vickrey [39] postulates that all travelers are identical in terms of "$\alpha - \beta - \gamma$" preferences. When deciding departure time, travelers make a trade-off between the travel cost in terms of travel delay and the schedule costs of arriving too early or too late at destinations so as to reach the UE. This indicates that the user cost is a linear function of travel time and schedule delays, see Section 2. Additionally, a demand curve (a relationship between the equilibrium user cost and the number of road users) may apply to determine the total number of trips.

In this study, we would like to demonstrate that the MFD shape of a particular network is strongly influenced by the departure time choices. The model proposed here constructs an MFD without topological information but solely with the use of (i) time series of the number of travelers who entered the network at a particular time and (ii) the UE assumptions and associated "$\alpha - \beta - \gamma$" preferences. With these two things, an MFD model emerges that indeed describes the reservoir dynamics of a particular network. Figure 3 shows the idea. The classic approach to reconstruct an MFD is to use traffic flow models [40, 41] to simulate traffic dynamics in a specific network topology. This approach can give MFDs associated with input demand profiles, showing impacts of the network topology and the demand profile. Our approach is different. Although—like in the classic approach—the demand profile is exogenous, by incorporating (an assumed) UE principle behind the demand profile, the shape of the MFD also naturally emerges. Our model can construct MFDs associated with an infinite number of demand profiles, which essentially creates a pool of pairs of demand profile and its associated MFD, which all satisfy the UE principle in departure time choices. In a specific city, the network topology (+ driving behavior as well as traffic rules and control) will determine which pair of demand profile and MFD in the pool is likely to be observed in reality.

The reasons to take a network-free approach, instead of using the classic simulation model, are threefold. First, in classic simulations, it is difficult to rule out impacts of network topology on the MFD shape. As shown in [42], the MFD needs to be determined for each network separately and cannot be derived from general properties. Second, it is cumbersome to run network-based simulations in a large network. Third, it is difficult to reach a stable UE in departure time choices in a network-based simulation. As argued in [43], a dynamic system for the stable UE in departure time choices is still missing. Recently, some dynamic systems for the UE in departure time choices have been proposed in [43, 44]. But these systems are only examined at a single bottleneck. Hence, to reach the goal of this paper, i.e., understanding the insight in the inconsistency between the empirical and theoretical MFD from the perspective of departure time choices, we propose the network-free approach.

The general line of thought in the paper is as follows. A demand profile (i.e., departure rate as a function of time) typically increases and then decreases as function of times. It can hence be represented by a function which for the sake of argument we simplify to the shape of a bell (probability density function characterized by means and standard deviation). By assuming UE in terms of departure time choice, we can reconstruct possible outflow curves. We then derive closed-form expressions of the traffic density and outflow, which are associated with the given demand profile. Using the density and outflow formula, the associated MFD emerges with the given departure time choices. This

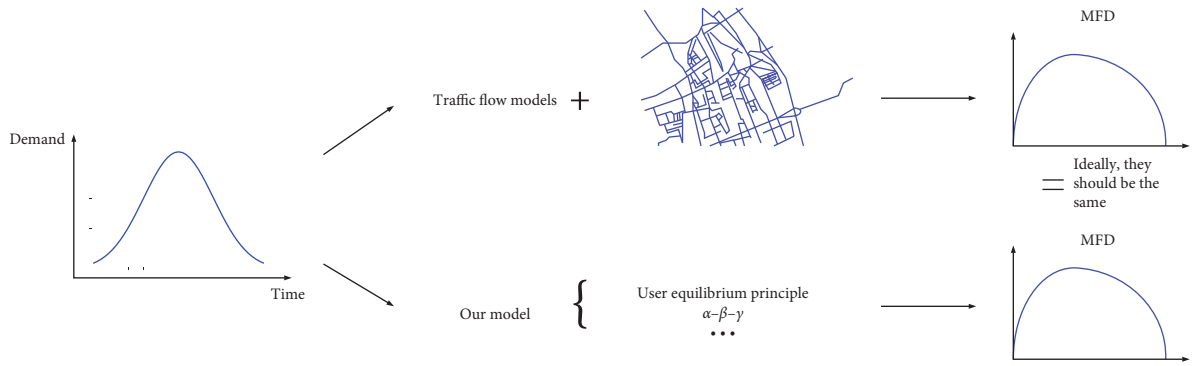

Figure 3: Two independent modeling processes to describe traffic dynamics. The MFDs given from these two modeling processes are expected to be consistent with each other.

approach allows us to conduct a sensitivity analysis of the MFD to the user cost parameters and the demand profile characteristics (i.e., mean and standard deviation). The analytical analysis can help us to understand how to calibrate parameters to give the expected MFD.

The main contribution is to understand the MFD shape and the mechanism behind its dependence on traffic demand. The approach is to investigate the inconsistency between the empirical and the theoretical MFD by proposing a network-free model. Our work shows that the hysteresis phenomenon is inevitable. In addition, our model shows how the density and outflow are shaped by the demand profile, and why the commonly used "S"-shaped cumulative departure rate curve cannot yield a congestion branch of the MFD. Our findings imply that the missing of congestion branch in empirical observations is a consequence of the user equilibrium in departure time choices, rather than an indicator of congestion severity. For urban traffic management purposes, our findings could benefit the evaluation of MFD-based control applications.

The remainder of the paper proceeds as follows. Section 2 describes the modeling approach to giving MFD from departure time distribution. Then, the impacts of departure time decision-making process on the MFD are shown qualitatively and quantitatively in Section 3 and Section 4, respectively. We end this paper with conclusions and discussions in Section 5.

2. Traffic Dynamics as a Result of Demand Profile and UE Assumptions

In this section, we propose close-form expressions of the network (reservoir) density and outflow, based on demand profiles and the UE principle. We consider a city as a single reservoir. All travelers would like to arrive at their destinations at the same time, t^*. The length of all trips is the same, denoted as l. The network size, L, is the total street length in the network.

The demand profile $\mathbb{D}$ depicts the cumulative curve of departures starting from initial time $t = 0$. We postulate that this demand profile is a consequence of the deterministic UE principle for departure time choices, which means that all travelers should have the same user cost, which consists of a combination of travel delay (due to congestion) and scheduled delays due to arriving too early or too late with respect to their preferred arrival time t^*. We assume all travelers are identical in terms of their "$\alpha - \beta - \gamma$" preferences, which means the cost per hour of earlier arrival than t^* (schedule delay early) is β and the cost per hour of later arrival (schedule delay late) is γ. The cost per hour of travel delay is α (which is also called the value of time throughout this paper). The user cost Z of every traveler is hence expressed as

$$Z = Z_i = \alpha \cdot \tau_i + \max\left(\beta \cdot \left(t^* - t_i^a\right), \gamma \cdot \left(t_i^a - t^*\right)\right), \quad (1)$$

where Z_i, τ_i, and t_i^a are the user cost, the travel delay, and the arrival time of the ith traveler, respectively. The travel delay τ_i is estimated as $\tau_i = t_i^a - t_i^d - \tau^f$ where t_i^d and τ^f are the ith traveler's departure time and free-flow travel time. Note that as consequence of the UE, the cost for all travelers is the same, and the travel cost for the ith traveler, Z_i, holds for all travelers.

Graphically, we can show elements of the user cost as in Figure 4. In the deterministic UE, the user cost of every trip is the same. Thus, according to (1), the relationship between the travel delay and the arrival time is linear, see Figure 4. As the arrival time approaches to the preferred arrival time by one time unit from the left (or right), the associated travel delay will increase accordingly by β/α (or γ/α respectively).

The earliest and latest arrival time are denoted by t_1 and t_2, respectively. Because the first and the last trip travel at free-flow speed, we can define the starting and ending time of the demand profile $\mathbb{D}$ as 0 and $t_2 - \tau^f$, respectively. The earliest arrival time is $t_1 = \tau^f$. The user cost of the trip arriving at t_1 is expressed as $Z = \beta(t^* - \tau^f)$. That equals the cost of other trips arriving earlier than t^*. That is, $\beta(t^* - \tau^f) = \alpha(t_i^a - t_i^d - \tau^f) + \beta(t^* - t_i^a)$. This allows us to express the arrival time t_i^a as a function of the departure time t_i^d:

$$t_i^a = \tau^f + \frac{\alpha t_i^d}{\alpha - \beta}, \quad \text{for } t_i^a \leqslant t^*. \quad (2)$$

Following a similar reasoning for trips arriving late, we have $\beta(t^* - \tau^f) = \alpha(t_i^a - t_i^d - \tau^f) + \gamma(t_i^a - t^*)$. Hence, the arrival time of trips arriving later than t^* can be expressed as

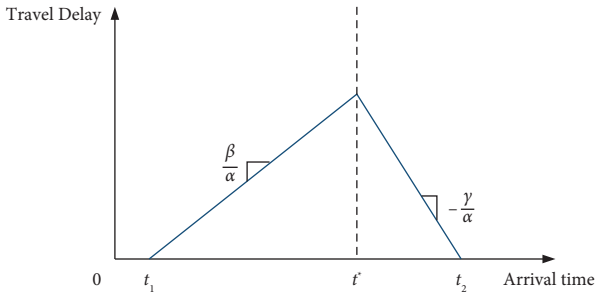

Figure 4: Linear relationship between travel delay and arrival time in user equilibrium.

$$t_i^a = \frac{(\beta+\gamma)t^* + \alpha t_i^d + (\alpha-\beta)\tau^f}{\alpha+\gamma}, \quad \text{for } t_i^a \geqslant t^*. \tag{3}$$

We can also formulate a relation between t_1 and t_2, i.e., $\beta(t^* - t_1) = \gamma(t_2 - t^*)$. The preferred arrival time can be derived endogenously as

$$t^* = \frac{\gamma t_2 + \beta t_1}{\beta+\gamma} \text{ where } t_1 = \tau^f. \tag{4}$$

For the next steps, we use the relation between the total demand and the user cost, i.e., the relationship that governs how many travelers we can expect given a particular total cost (as opposed to a simulation model that governs what costs we can expect given a total demand). We will assume a linear relationship in which the total demand, N, is a linear function of user cost Z, for example, the one depicted in Figure 5. The slope θ indicates how the equilibrium user cost affects the total user demand. Figure 5 is for illustration purposes only, and the sign of θ depends on changes considered. There might be two different types of changes. If one considers an exogenous increase in demand, the total demand and the user cost increase. If one considers an exogenous change in network capacity, the actual cost will go down and latent demand will increase the total demand. Following this line of the reasoning, we will only need the fact that they can be connected. Using the demand curve in Figure 5 as an example, we can express the user cost associated with the demand N as

$$Z = \theta(N - N_0), \tag{5}$$

where N_0 is a constant horizontal intercept. The relationship between the total demand and the user cost is frequently used by economists to study the elastic demand [45]. Clearly, the user cost in (5) should be consistent with (1), i.e., $Z = (t^* - \tau^f)\beta$. Combing (1) and (5) gives

$$N = \frac{(t^* - \tau^f)\beta}{\theta} + N_0. \tag{6}$$

Combining (4) and (6), we can reformulate the demand as a function of the demand period duration $t_2 - t_1$:

$$N = \frac{\gamma\beta(t_2 - t_1)}{\theta(\beta+\gamma)} + N_0. \tag{7}$$

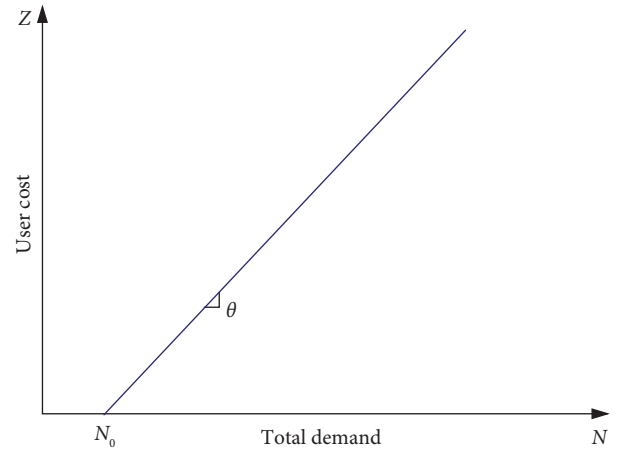

Figure 5: Demand curve. The relation is assumed to be linear. The constant θ is the slope of the demand curve and shows how the equilibrium user cost affects the user quantity demanded.

We assume the demand profile $\mathbb{D}$ is bounded within $[0, t_2 - \tau^f]$. Let us now estimate the departure function (in this paper, we will use the traffic engineering convention of demand representing the vehicles entering into the network and the vehicles arriving at their destination, hence leaving the network). We firstly consider a probability density function of departure time, $f(t^d)$ (e.g., normal distribution). The total demand, N, times the probability density at time t^d gives the departure rates at that time, i.e., $q(t^d)$. Then, we obtain the cumulative curve of departure rates $N_c^d(t^d)$:

$$N_c^d(t^d) = N \cdot F(t^d), \tag{8}$$

where $F(t^d)$ is the cumulative probability function of $f(t^d)$.

Figure 6 shows how to estimate the density using the departure and arrival cumulative curves. The vertical difference between the cumulative departure and arrival curve is the number of vehicles in the network. The density at time t^d, $k(t^d)$, is estimated as $N_c^d(t^d) - N_c^a(t^d)/L$. Consider a time $\tilde{t}^d$ that is implicitly defined by the time that cumulative departure rate $N_c^d(\tilde{t}^d)$ is equal to $N_c^a(t^d)$, see Figure 6. Travelers departing at time $\tilde{t}^d$ will reach their destinations at time t^d. The density will be expressed as

$$\begin{aligned} k(t^d) &= \frac{N_c^d(t^d) - N_c^a(t^d)}{L} \\ &= \frac{N_c^d(t^d) - N_c^d(\tilde{t}^d)}{L} \\ &= \frac{N}{L} \cdot \left(F(t^d) - F(\tilde{t}^d)\right), \end{aligned} \tag{9}$$

where $N = (\gamma\beta(t_2 - \tau^f))/(\theta(\beta+\gamma)) + N_0$ according to (7).

We can replace the arrival time t^a and the departure time t^d in (2) and (3) with t and $\tilde{t}$, respectively. Then, we can express the departure time $\tilde{t}$ as a function of the arrival time t:

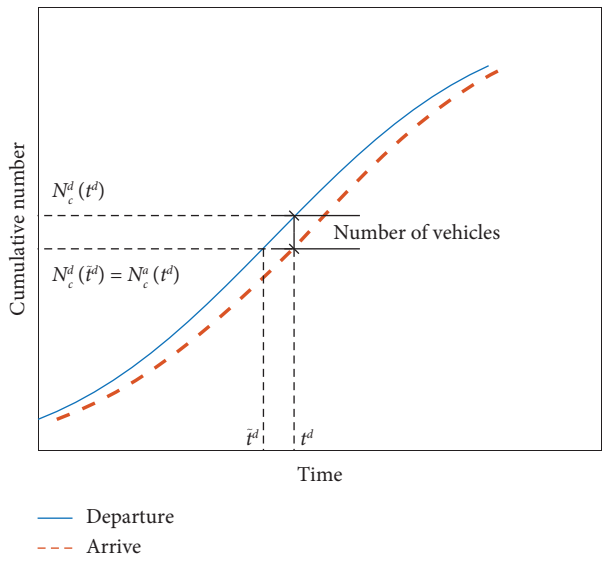

Figure 6: Cumulative curves of departure and arrival rates.

$$\tilde{t} = \frac{(\alpha-\beta)\left(t-\tau^f\right)}{\alpha}, \quad \text{for } t \leqslant t^*,$$
$$\tilde{t} = \frac{(\alpha+\gamma)t-(\beta+\gamma)t^*-(\alpha-\beta)\tau^f}{\alpha}, \quad \text{for } t \geqslant t^*. \tag{10}$$

When estimating the density at time t, we first derive $\tilde{t}$ using (10). According to the demand profile, we then have the cumulative departure rate at time t and $\tilde{t}$. Finally, the density will be given by (9).

We are also interested in the outflow. Basically, the outflow $q_{\text{out}}(t)$ is given by

$$\begin{aligned} q_{\text{out}}(t) &= \frac{\mathrm{d}N_c^a(t)}{\mathrm{d}t} \\ &= \frac{\partial N_c^d(\tilde{t})}{\partial \tilde{t}} \cdot \frac{\partial \tilde{t}(t)}{\partial t} \\ &= Nf(\tilde{t}) \cdot \frac{\mathrm{d}\tilde{t}(t)}{\mathrm{d}t}. \end{aligned} \tag{11}$$

The function $\tilde{t}(t)$ (i.e., (10)) does not have a derivative at $t = t^*$. Because time always increases in simulations, we estimate the derivative at time $t = t^*$ as the time t approaches t^* from the left. Substituting (10) into (11), we can have expressions of the outflow as

$$q_{\text{out}}(t) = Nf(\tilde{t}) \cdot \left(1-\frac{\beta}{\alpha}\right), \quad \text{for } t \leqslant t^*,$$
$$q_{\text{out}}(t) = Nf(\tilde{t}) \cdot \left(1+\frac{\gamma}{\alpha}\right), \quad \text{for } t > t^*, \tag{12}$$

where $N = (\gamma\beta(t_2-\tau^f))/(\theta(\beta+\gamma)) + N_0$ and $t^* = (\gamma t_2 + \beta\tau^f)/(\beta+\gamma)$ according to (4) and (7). The MFD plotted using expression (9) and (12) will be determined by a single parameter, t_2, and the demand profile distribution f. Note that the outflow and density are formulated as functions of time t, see (9) and (12). The density and outflow at time $t \leqslant t^*$ form an early arrival branch in the MFD; the states at time $t > t^*$ form a late-arrival branch.

Note that the outflow profile is discontinuous at time t^*, see (12). Physically, this is explained by a difference in value between being early and being late. From the mathematics, we can see that the late-arrival outflow (at time $t > t^*$) is higher than the demand at $\tilde{t}$ by a factor $1 + \gamma/\alpha > 1$ while the early arrival outflow (at time $t \leqslant t^*$) is lower than the demand at $\tilde{t}$ by a factor $1 - \beta/\alpha < 1$. When $t = t^*$, if $f(t)$ is continuous at time $\tilde{t}$, one could expect a jump of outflow at time t. Therefore, the outflow will be discontinuous at time t, and the late-arrival outflow is higher than the early arrival one.

Let us now consider the effect of the parameters on this property and the reason why many MFDs shown empirically might seem continuous. A much higher α (than β and γ), which means lower β/α and γ/α, indicates that travelers dislike traveling (and hence queuing) even more than arriving early or being late, respectively. That is expected to be realistic. Consider the demand $f(t)$ is continuous along time. According to (12), when β/α and γ/α are 0 (the limit of a very high α), the outflow will be continuous along time too. The low-value β/α and low-value γ/α may match with an empirical MFD that looks continuous. Relaxing the assumption of a fixed desired arrival time t^*, distributed desired arrival time might lead to a similar effect since it will smoothen the sudden transition from being early to being late.

3. Hysteresis Phenomenon in MFD: Qualitative Analysis

This section aims at qualitatively explaining how a demand profile determines the MFD shape. The section provides two main insights. It first clarifies why and how the demand profile gives more than one outflow values associated to the same density (i.e., the hysteresis phenomenon). Second, it explains from the perspective of departure time choices why the so-called congestion branch is rarely observed with empirical data.

Let us first analyze the MFD shape, and to this end, consider the density and outflow resulting from a typical demand profile, see Figure 7. At time t, a departure rate is denoted by $q^d(t)$. According to Section 2, the outflow at time t, $q_{\text{out}}(t)$, will be determined by two components: first, the departure rate at time $\tilde{t}$, $q^d(\tilde{t})$; second, whether the time t is earlier than the preferred arrival time or not. The time $\tilde{t}$ is estimated using (10). The area under the demand profile between time t and $\tilde{t}$ equals the number of vehicles in the network at time t (i.e., $k(t) \cdot L$).

Let us consider a typical demand profile, which increases firstly and then decreases along time, see Figures 8(a) and 9(a) for illustrations. In that case, the same outflow is observed at different time t_i and t_j, respectively. If $t_i < t_j < t^*$, according to (12), the inflow at $\tilde{t}_i$ and $\tilde{t}_j$ should be the same, see Figure 8(a). The corresponding densities are related to the area of the grey shading. We use number "1" and "2" to denote two traffic states observed at time t_i and t_j, respectively. For this demand pattern, we also construct the

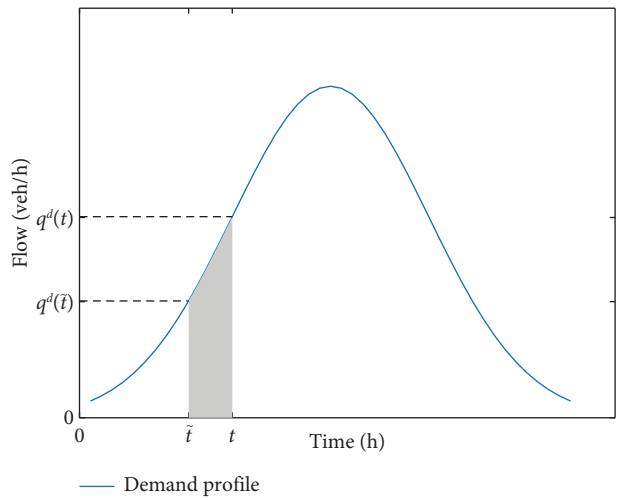

FIGURE 7: Illustrations of outflow and density in the demand profile.

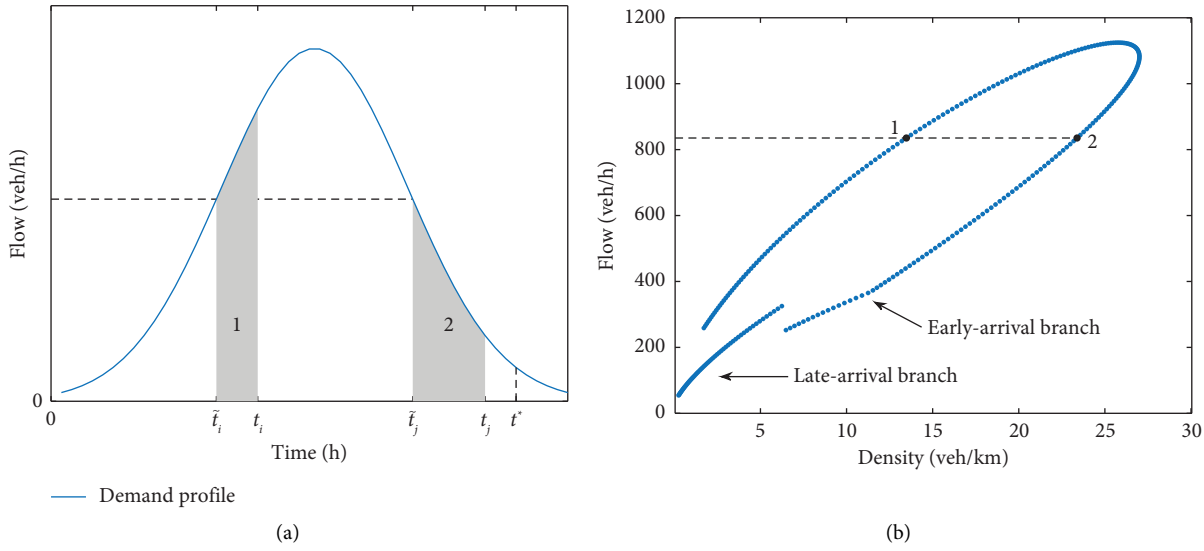

FIGURE 8: An illustration of hysteresis phenomenon when t_i and t_j are both earlier than the preferred arrival time t^*. To give the same outflow, the inflow at departure time $\tilde{t}_i$ and $\tilde{t}_j$ is the same, see (a). The shading illustrates density in different traffic states (denoted by different numbers). The MFD is given in (b). (a) Demand profile (when t_i and t_j are both earlier than the preferred arrival time t^*). (b) MFD showing the corresponding traffic states 1 and 2 (when t_i and t_j are both earlier than the preferred arrival time t^*).

MFD using the method as described, which is shown in Figure 8(b). The MFD shows two branches: early arrival and late-arrival branches. For the case in Figure 8(a), traffic states "1" and "2" are on the early arrival branch. If $t_i < t^* < t_j$ (i.e., the case shown in Figure 9(a)), to observe the same outflow at both t_i and t_j, the inflow q_j should be lower than q_i according to (12). The two illustrated traffic states are denoted by "3" and "4," respectively. They are depicted in the late-arrival branch of the MFD in Figure 9(b). Hence, for the same outflow, the associated density could be very different, which is considerably affected by the demand profile and the preferred arrival time t^*. As shown in Figure 8, the MFD emerges as a hysteresis loop structure—more than one corresponding density for a flow.

Lemma 1. *$t > \tilde{t}$. When $t \leqslant t^*$, the time duration between t and $\tilde{t}$ increases as time t increases; when $t > t^*$, the time duration between t and $\tilde{t}$ decreases as time t increases.*

Proof. According to (10), the duration $t - \tilde{t}$ can be expressed as follows:

$$t - \tilde{t} = \frac{\beta}{\alpha} \cdot t + \left(1 - \frac{\beta}{\alpha}\right) \cdot \tau^f, \quad \text{for } t \leqslant t^*,$$
$$t - \tilde{t} = \frac{-\gamma t + (\beta + \gamma) t^* + (\alpha - \beta)\tau^f}{\alpha}, \quad \text{for } t > t^*. \tag{13}$$

As time goes by, if the time $t \leqslant t^*$, the derivative $\mathrm{d}(t - \tilde{t})/\mathrm{d}t = \beta/\alpha > 0$ shows that the time duration increases as

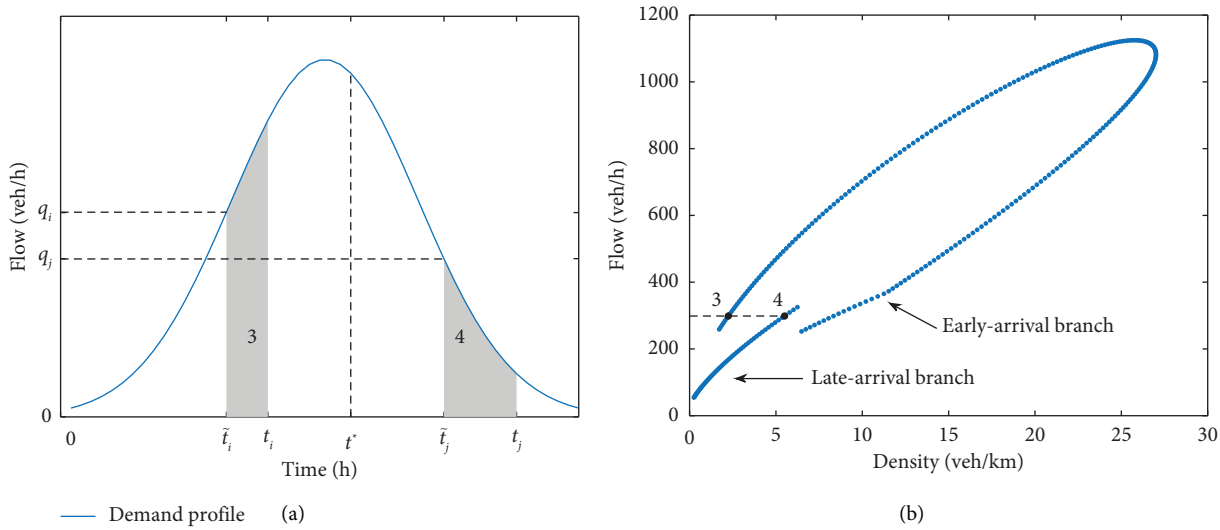

FIGURE 9: An illustration of hysteresis phenomenon when t_i and t_j are earlier and later than the preferred arrival time t^*, respectively. Given the same outflow, the associated densities can be different because of the demand profile shape. The shading illustrates density in different traffic states (denoted by different numbers). (a) Demand profile (when t_i and t_j are earlier and later than the preferred arrival time t^*, respectively). (b) MFD showing the corresponding traffic states 3 and 4 (when t_i and t_j are earlier and later than the preferred arrival time t^*, respectively).

time goes by; if the time $t > t^*$, $\mathrm{d}(t - \tilde{t})/\mathrm{d}t = -\gamma/\alpha < 0$ means the time duration decreases.

Substituting (4) for t^* in (13), we can see when $t > t^*$, $t - \tilde{t} = \gamma/\alpha(t_2 - t) + \tau^f$. Because $t \leqslant t_2$ and $\alpha, \gamma > 0$, we can derive that $t - \tilde{t} > \tau^f > 0$. Hence, we can conclude that the time used to estimate the outflow (i.e., $\tilde{t}$) is always in the left of time t, that is, $t > \tilde{t}$. □

Consider a traffic state transition along congestion branch, i.e., as time goes on, the density increases while the outflow decreases. According to (12), if $q_{\mathrm{out}}(t)$ decreases, then accordingly $f(\tilde{t})$ should decrease. The expected realistic demand profile is "S"-shaped (i.e., demand increases and then decreases along time). So, we can conclude that if the outflow decreases as time goes on, the departure time t and the corresponding arrival time $\tilde{t}$ both should have passed the time when demand reaches its peak (i.e., on the right-hand decreasing branch of the demand profile). As shown in Figure 9(a), the density corresponds to the shaded area below the right-hand demand branch. As time passes, the shaded area moves to the right (the left-hand tail of the shaded will disappear, and new shaded area will be added at the right-hand side). If $t_j > t^*$ (see state 4 in Figure 9(a)), the temporal duration of the shaded (or called "shading width") decreases as t_j increases, see Lemma 1 and (13). Given the S-shaped demand cumulative curve, the shaded area will decrease along time when $t_j > t^*$. That is, in the traffic state transition along the late-arrival branch, when the outflow decreases, the density will decrease. That is inconsistent with the traffic state transition along the congestion branch.

Hence, if a congestion branch existed, it should be on the early arrival branch. Consider the traffic state transition along the congestion branch from low density to high density (e.g., state 2 in Figure 8(a)). On the early arrival branch, when time increases by Δt, $\tilde{t}_j$ will accordingly increase by $(1 - \beta/\alpha)\Delta t$, see (13). Only if the area in time duration $[\tilde{t}_j, \tilde{t}_j + (1 - \beta/\alpha)\Delta t]$ is smaller than the area in time duration $[t_j, t_j + \Delta t]$, the density increases along time. As such, to observe an increasing density when outflow decreases, β/α is required to be close to 1 (minimizing the disappeared shaded area). However, as argued in Section 2, β/α (lower than 1) is more reasonable (because many travelers prefer departing earlier or later to avoid traffic congestion in real life). Hence, it is rare to observe the congestion branch. When the outflow is very low, the associated density will be small. That also explains why we will observe hysteresis loops rather than a complete concave MFD. Numerical examples are given in Figures 8 and 9. As the density increases along time, the outflow would increase; when the density decreases, the outflow would decrease as well. Hence, there is no congestion branch in the MFD shown in Figures 8 and 9.

4. Numerical Illustration of MFD Associated with Demand Profile

In this section, we show the phenomena presented in previous sections numerically. The numerical case study has three purposes: (i) numerically depicting the MFD; (ii) testing whether we can observe the hysteresis phenomenon and the congestion branch; and (iii) evaluating sensitivity of the MFD to different input parameters.

We will hence do the numerical implementation for a variety of demand profiles to test the sensitivity of the MFD shape to the demand. According to Section 2, the MFD shape is determined by the probability density function of the departure time, the latest arrival time t_2 (or the rush hour duration), and user cost parameters α, β, and γ. We describe the setup of the numerical experiment in Section 4. The illustration results are presented in Section 4.

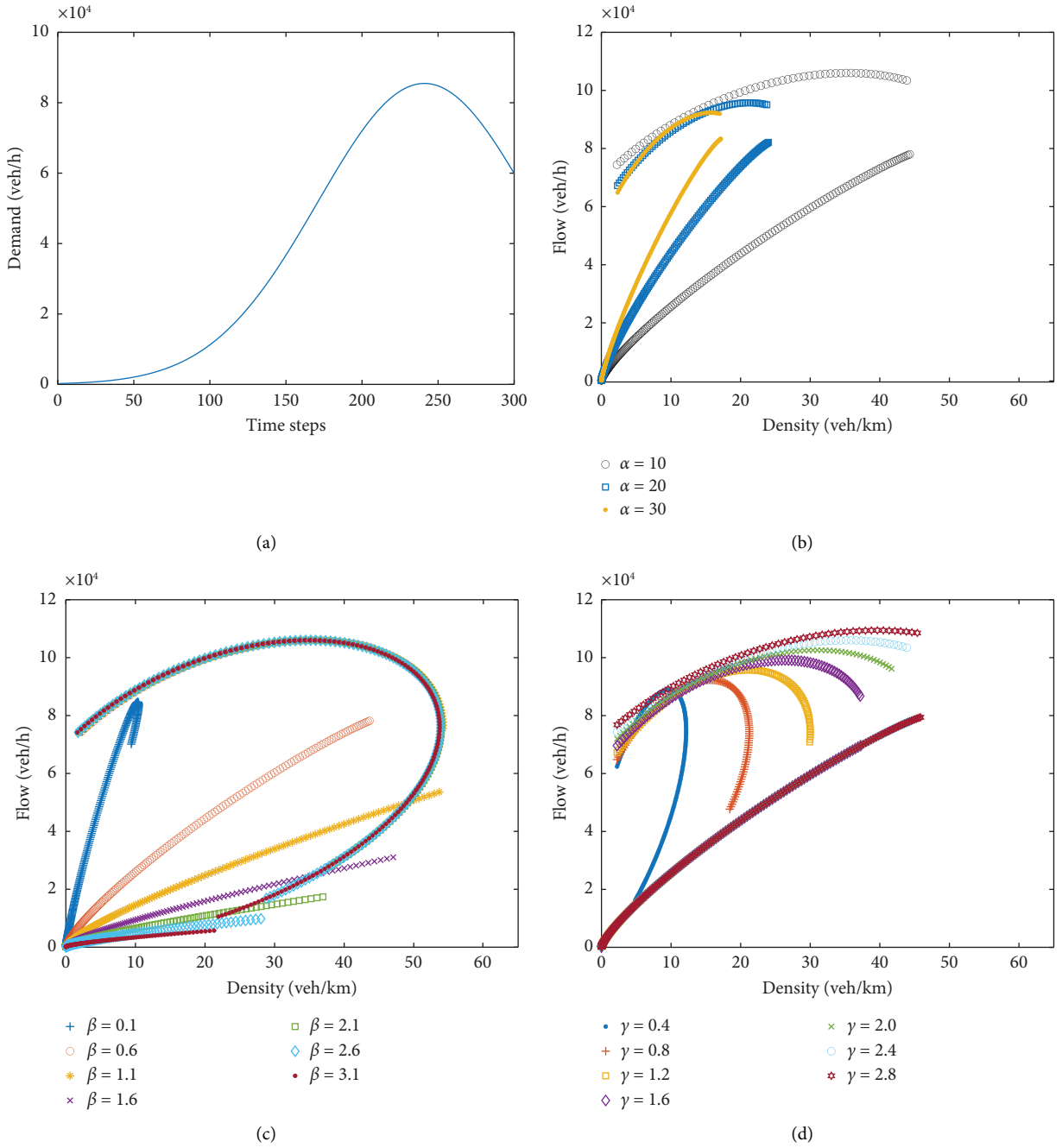

FIGURE 10: Sensitivity analysis of the MFD to the parameters α, β, and γ. The demand profile is shown in (a). The MFDs are given in the remaining three subfigures. (a) Demand profile that follows a normal distribution with mean $\mu = 240$ and standard deviation $\sigma = 70$. (b) Sensitivity of the MFD to the parameter α. $\beta = 0.61$ and $\gamma = 2.4$. (c) Sensitivity of the MFD to the parameter β. $\alpha = 10$ and $\gamma = 2.4$. (d) Sensitivity of the MFD to the parameter γ. $\alpha = 10$ and $\beta = 0.61$.

4.1. Setup. This section describes the numerical case study setup. The demand profile describes the departure rate during the rush hour (from 0 to $t_2 - \tau^f$). We can have $F(0) = 0$ and $F(t_2 - \tau^f) = 1$. When formulating the demand profile, we first assume a normal distribution $f_N(t)$ characterized by mean μ and standard deviation σ. The probability density function of departure time during the rush hour is estimated as $f(t) = f_N(t)/[F_N(t_2 - \tau^f) - F_N(0)]$. If t_2 is fixed, the mean value and standard deviation of f should increase/decrease as μ and σ increase/decrease. The total road length in the network is $L = 500$ km. Trip length l is 2 km. Time is discretized into several steps of 1 min. We estimate the density and outflow every time step.

We design a reference scenario where the parameter values in the user cost function are given as follows: $\alpha = 10$, $\beta = 0.61$, and $\gamma = 2.4$. The ratio of these parameters is loosely based on [46]. For the demand curve, $\theta = -50$ and $N_0 = 200,000$ veh. To fix demand, we initially choose a rush-

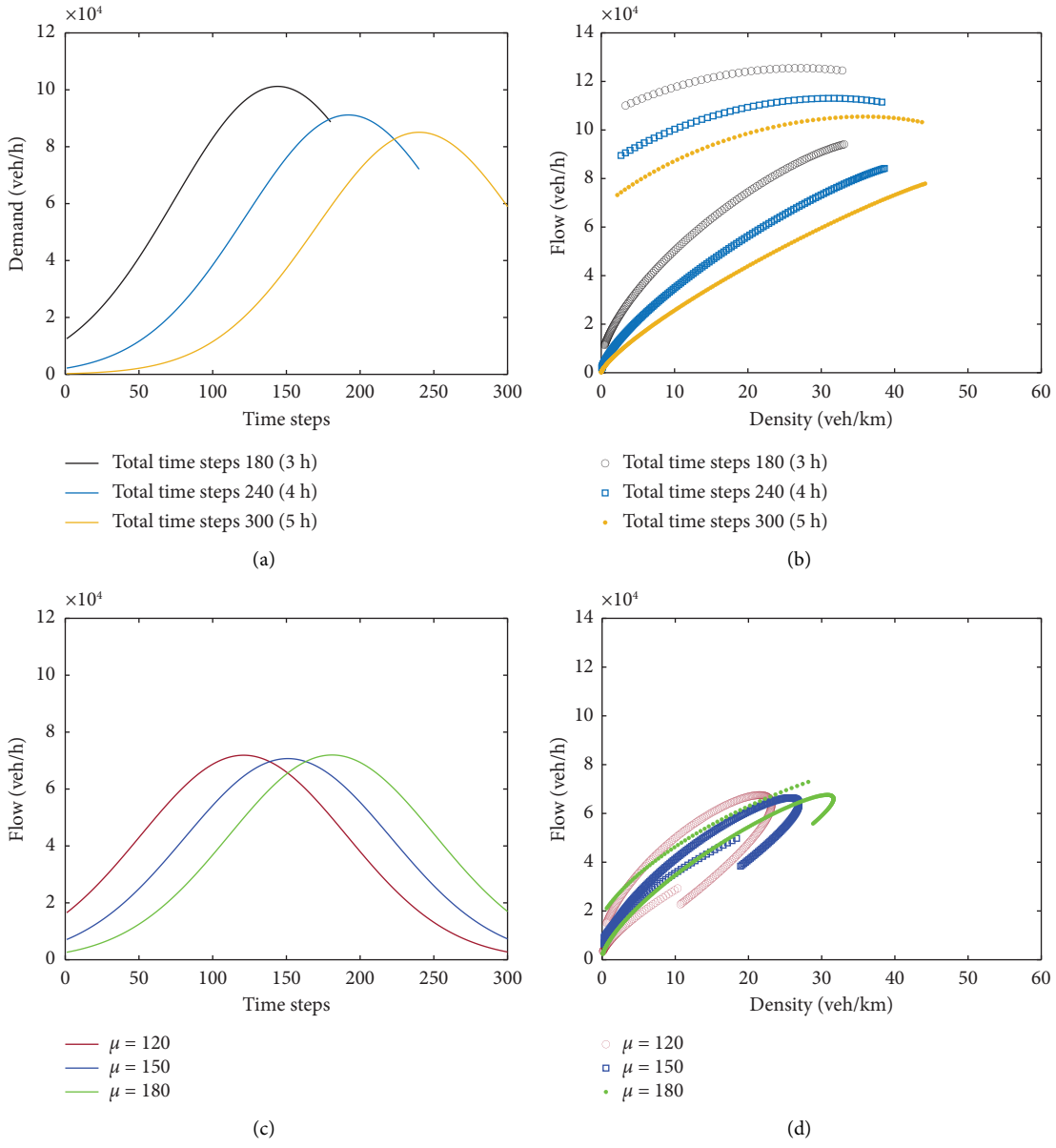

Figure 11: Continued.

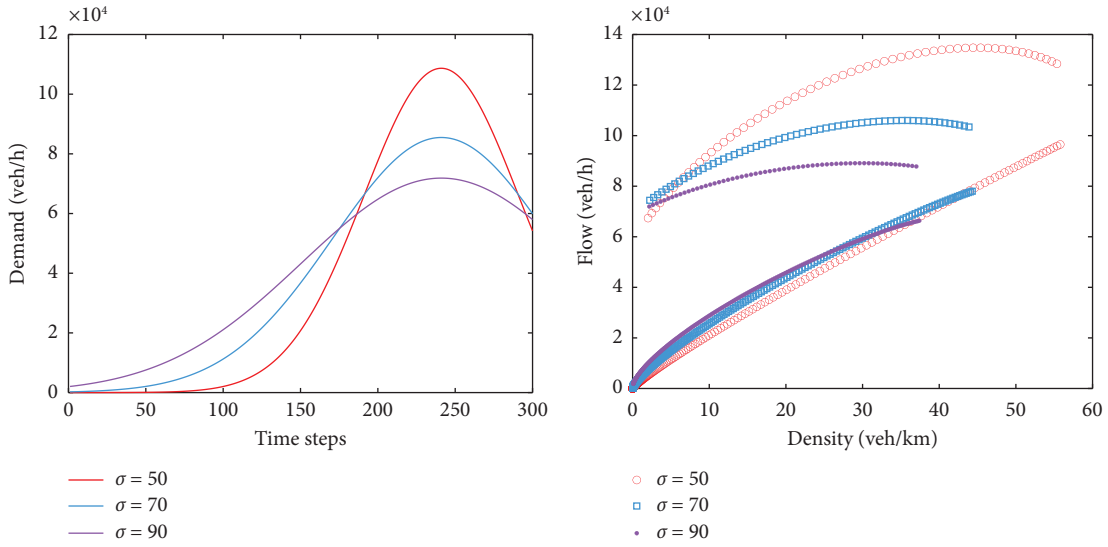

Figure 11: Sensitivity analysis of the MFD to demand profiles. The demand profiles are given in the left-hand column, i.e., (a), (c), and (e). The associated MFDs are given in the right-hand column i.e., (b), (d), and (f). (a) Demand profile that follows a normal distribution with mean $\mu = 0.8 * (t_2 - \tau^f)$ and standard deviation $\sigma = 70$. (b) Sensitivity of the MFD to the parameter t_2. The hysteresis loops are counterclockwise. (c) Demand profile that follows a normal distribution with standard deviation $\sigma = 70$ and different μ values. (d) Sensitivity of the MFD to the parameter μ. $\sigma = 70$. (e) Demand profile that follows a normal distribution with mean $\mu = 240$ and different σ values. (f) Sensitivity of the MFD to the parameter σ. $\mu = 240$.

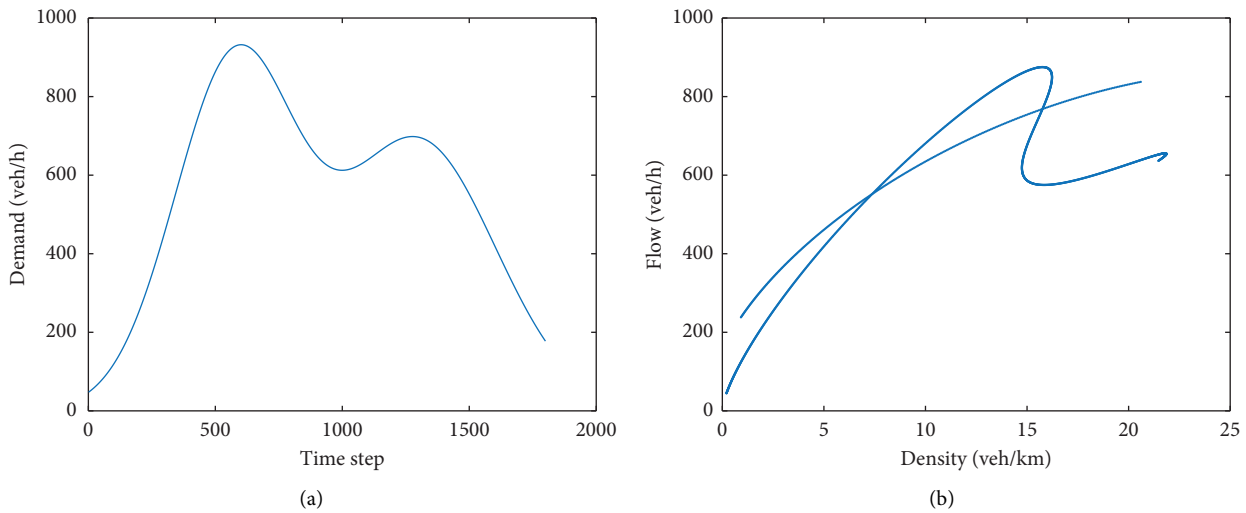

Figure 12: Continued.

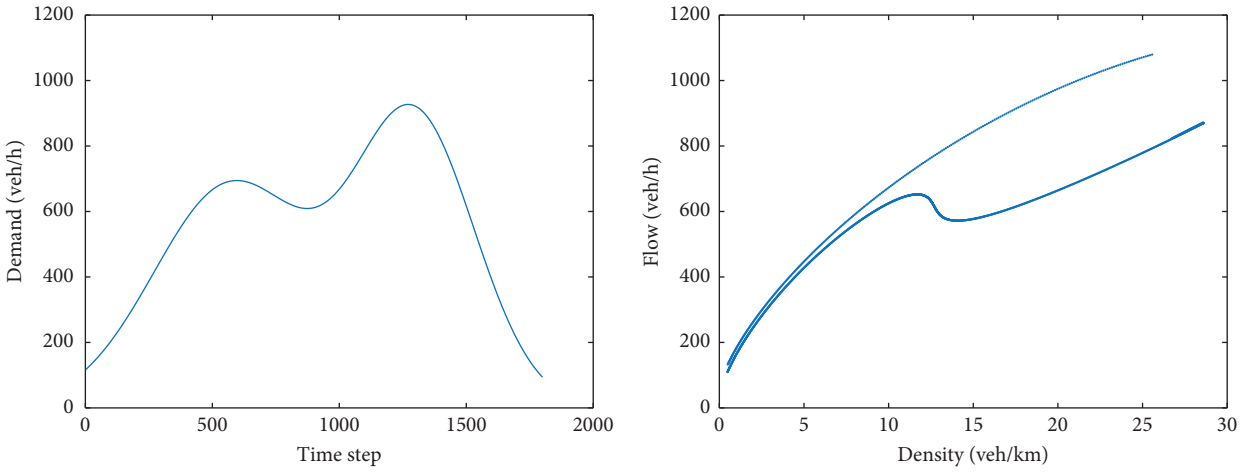

Figure 12: Different types of distributions were attempted, but the congestion branch still cannot be reproduced. The bimodal distribution is used to formulate the demand in (a) and (c). (a) One example of a bimodal demand profile. (b) Hysteresis in MFD, emerging from the demand profile in (a). (c) The other example of a bimodal demand profile. (d) Hysteresis in MFD, emerging from the demand profile in (c).

hour duration of 5 hours, and further $\mu = 150$ and $\sigma = 70$. Variations thereof will also be considered.

4.2. Results. In this section, given demand profiles, we generate associated MFDs using our model. We depict MFDs that match with different input parameters (t_2, μ, σ, α, β, and γ) and demand profiles.

4.3. Overall Shape. First, we analyze the overall shape. We see that the MFD consists of two branches: early arrival and late-arrival branch. In Figures 10 and 11, none of the depicted MFDs show a congested branch (i.e., decreasing outflow with increasing density). Both the early arrival branch and late-arrival branch form hysteresis loops. The MFDs are discontinuous as expected because the outflow is not continuous along time at time t^*. This is in line with the theory developed in the previous section. We find as well, as also depicted in Figure 10(b), that the MFD seems more and more "continuous" or connected as α goes up.

Note here that the MFDs generated in Figures 10 and 11 are indeed different from empirical and theoretical ones in the literature. The reason could be that the demand profile in the numerical case study is given exogenously following a shape of the normal distribution for simplicity. Despite the difference between the generated MFD in our model and the empirical ones, we would like to highlight a finding that the congestion branch cannot be observed, regardless of demand profiles. In fact, several different types of distributions (e.g., bimodal distribution) were attempted, but the congestion branch still cannot be reproduced, see Figure 12. It means that the hysteresis is a result of UE in departure time choices.

Furthermore, note that all MFDs in Figure 10(b) reveal counterclockwise hysteresis loops. The average speed is a weighted ratio between outflow and density by l/L. Figure 10(b) shows that the speed of early arrivals increases as α raises. Early arrival travelers tend to spend less time on roads. On the contrary, the increasing β decreases the speed of early arrivals, see Figure 10(c). The late-arrival outflow function is independent of β. So, late-arrival branches in Figure 10(c) overlap with each other, shown as one concave curve at the top. Figure 10(d) shows how the MFD varies as γ increases. When $\gamma = 0.4$, the MFD is shown as a quite continuous counterclockwise loop. When γ increases, the early and late-arrival branches are more separated.

4.4. Effects of Demand Profile. Let us now focus on the effects of the demand profile on the MFD. The demand profile is characterized by three parameters, i.e., t_2, μ, and σ. We varied all three, and the resulting MFDs are shown in Figure 11. Below, we will comment on each of the parameters.

(i) In the simulations, the MFD associated with a higher t_2 (i.e., a longer rush hour duration) has lower capacity and slower speed. Different latest arrival time t_2 means different rush hour time duration. The corresponding MFDs are given in Figure 11(b), shown as counterclockwise hysteresis loops. In our numerical simulations, the demand profile is defined by normal distribution parameters, i.e., $\mu = 0.8\,(t_2 - \tau^f)$ and $\sigma = 70$. The mean value of the departure time is always at 80% of the rush hour duration. We simulate rush hours 3 h, 4 h, and 5 h. A longer rush hour means the probability density $f\,(t^d)$ at time t^d would be lower. The demand at time t^d would be lower, see Figure 11(a). Note here that by carefully choosing a positive θ, the total demand could increase with an increasing rush hour duration. Then, the impacts of the rush hour on the MFD could differ.

(ii) A higher mean value μ (i.e., the demand peak happens later) gives a higher late-arrival branch.

Note here that the mean value of the departure time is μ/A where $A = F_N(t_2 - \tau^f) - F_N(0)$ is a constant. A lower μ means most of the travelers would like to depart earlier. Hence, the late-arrival MFD branch will be lower as μ decreases. In numerical studies, the rush hour time duration is 5 hours, and the standard deviation $\sigma = 70$. The demand profiles associated with different mean value μ are shown in Figure 11(c). The associated MFDs are shown in Figure 11(d). The hysteresis loops for $\mu = 120$ and $\mu = 150$ are clockwise. When the mean $\mu = 180$, we can see a figure-of-eight hysteresis loop. As μ increases up to 240, the hysteresis loop will be counterclockwise (see squares in Figure 11(f)).

(iii) Additionally, a higher standard deviation σ (i.e., the demand is more evenly distributed over the rush hour duration) corresponds to a lower MFD capacity and a smaller critical density. The standard deviation of the departure time should be σ/A. A lower σ means the demand is more aggregated to a peak-hour instant (e.g., because the network has a higher capacity to evacuate a larger number of vehicles). A traffic demand would be more evenly distributed as σ goes up. Figure 11(e) shows demand profiles with different σ values. Accordingly, the associated MFDs are given in Figure 11(f).

5. Conclusions

This paper explores the shape of the MFD and explains the shapes as found in empirical works by a theoretical approach. We are particularly interested in the mechanism behind (1) the missing of the congestion branch and (2) the hysteresis. In this paper, the terminology "congestion" is used to describe the MFD branch where the flow decreases as the density increases. The other MFD branch in which flow increases as the density increases is called the free-flow branch. In the literature, the terms "free-flow" and "congestion" are sometimes referred to as "congestion" and "hypercongestion," respectively.

To reach the goal, a network-free approach is taken. We consider a large-area urban traffic network as one reservoir. The demand is described as departure rates along time, regardless of OD spatial distribution (or OD structure). In the trip scheduling decisions, departure time choices are assumed to be in line with the deterministic user equilibrium (UE) principle. This implies that the cost of all users is the same. The user trip cost is calculated with linear terms for travel time and early and late arrivals, using the conventional "$\alpha - \beta - \gamma$" approach. Via a demand curve, we show the relation between the user cost and total demand. Based on these considerations, we formulate the density and outflow expressions along time. The MFD is given as a relation between the density and the outflow. The model proposed in this paper shows a correlation between the demand profile and the MFD.

Our main conclusion is that the *hysteresis* phenomenon and the missing of the congestion branch are consequences of the UE in departure time choices. This explains why we can observe congestion branch in simulations when not considering UE in departure time choices, while in empirical observations, we can only see the hysteresis phenomenon. This conclusion also implies that in real life, travelers are quite rational when making trip decisions, consistent with the classic UE theory and the stability in traffic congestion patterns [43, 44]. Note here that this conclusion is different from ideas on the conditions for an MFD, namely, that the states in an MFD are stationary. This demand-dependent MFD definition is consistent with recent literature [11, 24].

To the best of the authors' knowledge, it is the first time to show that the missing of congestion branch is a result of the UE, rather than an indicator of congestion severity. The missing of congestion branch in MFD has already been demonstrated in quite a lot of empirical observations. Some may argue that the MFD with free-flow branch only (i.e., without the congestion branch) means the city is not oversaturated. As discussed in Section 1, a demand that is not sufficiently high was still considered as a possible reason for the missing of congestion branch. Following that argument, the delay might be still too small to present the congestion branch. But in real life, in a congested city, it is not so convincing to argue that the demand is not sufficiently high. Our study proposes an alternative reason, i.e., the missing of congestion branch is a property regardless of delays.

Some may argue that our research links the demand and the rush hour duration. The congestion cannot be presented because of a long rush hour duration, during which the network is filled and emptied. However, we would argue that, as shown in Figure 4, the maximum, average, and total delays would also increase as the rush hour duration increases. Consider a rather high demand (compared to the network capacity). This high demand would result in a very long rush hour duration. It is necessary to remark here that the delays in the city would also be rather large; otherwise, the rush hour duration would not be so long. Hence, the large delays which in fact indicate the congestion severity cannot be visualized as a congestion state in the MFD. That is, as the UE is applicable, the congestion branch of MFD will not be observed regardless of delays, total number of commuters, and the congestion severity.

Previous research has already noticed that the spatial density heterogeneity can affect the MFD but did not explain why this would happen. It can be argued that the spatial density heterogeneity is a result of travel behavior, such as departure time choices. The demand pattern, as a result of departure time choices, determines the queue dynamics (e.g., shock wave propagation and queue length) and hence an uneven spatial density distribution. Our work explains how the departure time choices shape the MFD, which also shed light on how the demand profile determines the spatial density heterogeneity.

This research is conducted in a one-reservoir framework. The possible complex OD matrix is aggregated as one demand profile. That means, in the proposed network-free approach, all travelers are considered as a single group. This one-reservoir modeling framework, focusing on aggregate behavior and ignoring details, is consistent with the existing

MFD-based parsimonious modeling principles. We realize that the aggregate modeling principle may underestimate the impacts of heterogeneity (e.g., in trip distance) on traffic dynamics. As argued in [18], the OD matrix could considerably affect the macroscopic traffic dynamics in a given network. However, we would argue that by ruling out the heterogeneity and isolating the UE in departure time choices, this paper can clearly present the impacts of UE in departure time choices on the MFD shape. As concluded in this paper, excluding the impacts of heterogeneity, the UE in departure time choices could explain the missing of the congestion branch. That is very important for urban traffic management.

In this research, the desired arrival time is the same for all travelers. Compared to a heterogeneous desired arrival time case, the uniform desired arrival time assumption maximizes the total travel time (and delays) in the network. The uniform desired arrival time assumption in this paper indicates that, even with the maximized total travel time, the MFD does not show a congestion branch.

As the next steps in this research, we envisage using this modeling approach for trip scheduling with stochastic UE principle and heterogeneity in value of time α. It is also important to conduct real-world testing and calibrations to validate our network-free analysis. In the future, our approach can also be extended to study how the heterogeneity (preferably based on data) of preferred arrival time influences traffic dynamics (e.g., spatial density heterogeneity). These future extensions will extend the current principles into a more realistic model, showing the abilities and limitations of our current analysis. For traffic management, our work possibly can contribute to better assessing MFD-based control applications (e.g., perimeter control).

Data Availability

No data were used to support this study.

Conflicts of Interest

The authors declare that they have no conflicts of interest.

Acknowledgments

This work was jointly supported by the National Natural Science Foundation of China (grant no. 72201088) and the Fundamental Research Funds for the Central Universities of China (grant no. PA2022GDSK0040), which are gratefully acknowledged.

References

[1] H. S. Mahmassani, M. Saberi, and A. Zockaie, "Urban network gridlock: theory, characteristics, and dynamics," *Transportation Research Part C: Emerging Technologies*, vol. 36, pp. 480–497, 2013.

[2] R. Herman and I. Prigogine, "A two-fluid approach to town traffic," *Science*, vol. 204, no. 4389, pp. 148–151, 1979.

[3] N. Geroliminis and C. F. Daganzo, "Existence of urban-scale macroscopic fundamental diagrams: some experimental findings," *Transportation Research Part B: Methodological*, vol. 42, no. 9, pp. 759–770, 2008.

[4] C. Buisson and C. Ladier, "Exploring the impact of homogeneity of traffic measurements on the existence of macroscopic fundamental diagrams," *Transportation Research Record*, vol. 2124, no. 1, pp. 127–136, 2009.

[5] V. L. Knoop, P. B. C. van Erp, L. Leclercq, and S. P. Hoogendoorn, "Empirical mfds using google traffic data," in *Proceedings of the 2018 21st International Conference on Intelligent Transportation Systems (ITSC)*, Maui, HI, USA, November 2018.

[6] F. Carlos, "Daganzo. "Urban gridlock: macroscopic modeling and mitigation approaches"," *Transportation Research Part B: Methodological*, vol. 41, no. 1, pp. 49–62, 2007.

[7] M. Amin, N. Geroliminis, and D. Helbing, "The spatial variability of vehicle densities as determinant of urban network capacity," *Philosophical Transactions of the Royal Society A*, vol. 368, 2010.

[8] V. L. Knoop, H. van Lint, and S. P. Hoogendoorn, "Traffic dynamics: its impact on the macroscopic fundamental diagram," *Physica A: Statistical Mechanics and Its Applications*, vol. 438, pp. 236–250, 2015.

[9] V. V. Gayah and C. F. Daganzo, "Clockwise hysteresis loops in the macroscopic fundamental diagram: an effect of network instability," *Transportation Research Part B: Methodological*, vol. 45, no. 4, pp. 643–655, 2011.

[10] C. F. Daganzo, V. V. Gayah, and E. J. Gonzales, "Macroscopic relations of urban traffic variables: bifurcations, multivaluedness and instability," *Transportation Research Part B: Methodological*, vol. 45, no. 1, pp. 278–288, 2011.

[11] L. Leclercq and M. Paipuri, "Macroscopic traffic dynamics under fast-varying demand," *Transportation Science*, vol. 53, no. 6, pp. 1526–1545, October 2019.

[12] J. P. Schorr, H. Samer, S. Kang, K. Jang, and H. Kachouch, "From structural equation modeling to macroscopic fundamental diagrams: investigating the impact of road segments safety on network level efficiency," in *Proceedings of the Road Safety on Five Continents (RS5C): 17th International Conference*, Rio de Janeiro, Brazil, May 2016.

[13] A. Loder, L. Ambühl, M. Menendez, and K. W. Axhausen, "Empirics of multi-modal traffic networks – using the 3D macroscopic fundamental diagram," *Transportation Research Part C: Emerging Technologies*, vol. 82, pp. 88–101, 2017.

[14] Y. Huang, N. Garrick, and K. W. Axhausen, "Evaluating shanghai's non-local vehicle restriction policy using the empirical macroscopic fundamental diagram," in *In Proceedings of the 18th Swiss Transport Research Conference*, Ascona, May 2018.

[15] L. Ambühl, A. Loder, M. C. J. Bliemer, M. Menendez, and K. W. Axhausen, "Introducing a re-sampling methodology for the estimation of empirical macroscopic fundamental diagrams," *Transportation Research Record*, vol. 2672, no. 20, pp. 239–248, 2018.

[16] A. Loder, L. Ambühl, M. Menendez, and K. W. Axhausen, "Understanding traffic capacity of urban networks," *Scientific Reports*, vol. 9, no. 1, Article ID 16283, 2019.

[17] R. Aghamohammadi and J. A. Laval, "Parameter estimation of the macroscopic fundamental diagram: a maximum likelihood approach," *Transportation Research Part C: Emerging Technologies*, vol. 140, Article ID 103678, 2022.

[18] L. Leclercq, C. Parzani, V. L. Knoop, J. Amourette, and S. P. Hoogendoorn, "Macroscopic traffic dynamics with heterogeneous route patterns," *Transportation Research Part C: Emerging Technologies*, vol. 59, pp. 292–307, 2015.

[19] C. F. Daganzo and N. Geroliminis, "An analytical approximation for the macroscopic fundamental diagram of urban traffic," *Transportation Research Part B: Methodological*, vol. 42, no. 9, pp. 771–781, 2008.

[20] J. A. Laval and F. Castrillón, "Stochastic approximations for the macroscopic fundamental diagram of urban networks," *Transportation Research Part B: Methodological*, vol. 81, pp. 904–916, 2015.

[21] L. Leclercq and N. Geroliminis, "Estimating mfds in simple networks with route choice," *Procedia-Social and Behavioral Sciences*, vol. 80, pp. 99–118, 2013.

[22] K. Yuan, V. L. Knoop, and S. P. Hoogendoorn, "Multi-class traffic flow on a partially space-shared road," *Transportation Business: Transport Dynamics*, vol. 7, no. 1, pp. 1505–1520, 2019.

[23] L. Ambühl, A. Loder, M. C. Bliemer, M. Menendez, K. W. Axhausen, and K. W. Axhausen, "A functional form with a physical meaning for the macroscopic fundamental diagram," *Transportation Research Part B: Methodological*, vol. 137, pp. 119–132, 2020.

[24] L. Ambühl, A. Loder, L. Leclercq, and M. Menendez, "Disentangling the city traffic rhythms: a longitudinal analysis of mfd patterns over a year," *Transportation Research Part C: Emerging Technologies*, vol. 126, Article ID 103065, 2021.

[25] W. Vickrey, "Congestion in midtown manhattan in relation to marginal cost pricing," *Economics of Transportation*, vol. 21, Article ID 100152, 2020.

[26] K. A. Small and X. Chu, "Hypercongestion," *Journal of Transport Economics and Policy*, vol. 37, no. 3, pp. 319–352, 2003.

[27] N. Geroliminis and D. M. Levinson, "Cordon pricing consistent with the physics of overcrowding," in *Transportation and Traffic Theory 2009: Golden Jubilee: Papers Selected for Presentation at ISTTT18, a Peer Reviewed Series since 1959*, W. H. K. Lam, S. C. Wong, and H. K. Lo, Eds., Springer, Boston, MA, USA, 2009.

[28] R. Arnott, "A bathtub model of downtown traffic congestion," *Journal of Urban Economics*, vol. 76, pp. 110–121, 2013.

[29] M. Fosgerau, "Congestion in the bathtub," *Economics of Transportation*, vol. 4, no. 4, pp. 241–255, 2015.

[30] R. Arnott, A. Kokoza, and M. Naji, "Equilibrium traffic dynamics in a bathtub model: a special case," *Economics of Transportation*, vol. 7-8, pp. 38–52, 2016.

[31] R. Lamotte and N. Geroliminis, "The morning commute in urban areas with heterogeneous trip lengths," *Transportation Research Part B: Methodological*, vol. 117, pp. 794–810, 2018.

[32] R. Arnott and J. Buli, "Solving for equilibrium in the basic bathtub model," *Transportation Research Part B: Methodological*, vol. 109, pp. 150–175, 2018.

[33] C. Li and H. Huang, "Analysis of bathtub congestion with continuous scheduling preference," *Research in Transportation Economics*, vol. 75, pp. 45–54, 2019.

[34] M. Johari, M. Keyvan-Ekbatani, L. Leclercq, D. Ngoduy, and H. S. Mahmassani, "Macroscopic network-level traffic models: bridging fifty years of development toward the next era," *Transportation Research Part C: Emerging Technologies*, vol. 131, Article ID 103334, 2021.

[35] J. G. Wardrop, "Some theoretical aspects of road traffic research," *Proceedings of the Institute of civil engineering*, vol. 1, 1952.

[36] Z.-C. Li, H.-J. Huang, and H. Yang, "Fifty years of the bottleneck model: a bibliometric review and future research directions," *Transportation Research Part B: Methodological*, vol. 139, pp. 311–342, 2020.

[37] M. Ameli, M. S. S. Faradonbeh, J.-P. Lebacque, H. Abouee-Mehrizi, and L. Leclercq, "Departure time choice models in urban transportation systems based on mean field games," *Transportation Science*, vol. 56, no. 6, pp. 1483–1504, 2022.

[38] W.-L. Jin, "Generalized bathtub model of network trip flows," *Transportation Research Part B: Methodological*, vol. 136, pp. 138–157, 2020.

[39] W. Vickrey, "Congestion theory and transport investment," *The American Economic Review*, vol. 59, 1969.

[40] G. Mariotte, L. Leclercq, and J. A. Laval, "Macroscopic urban dynamics: analytical and numerical comparisons of existing models," *Transportation Research Part B: Methodological*, vol. 101, pp. 245–267, 2017.

[41] V. L. Knoop and S. P. Hoogendoorn, "An area-aggregated dynamic traffic simulation model," *European Journal of Transport and Infrastructure Research*, vol. 15, pp. 226–242, 2015.

[42] V. L. Knoop, David de Jong, P. Serge, and Hoogendoorn, "Network fundamental diagrams and their dependence on network topology," in *Mohcine Chraibi, Maik Boltes, Andreas Schadschneider and Armin Seyfried*, pp. 585–590, Springer International Publishing, Cham, 2015.

[43] W.-L. Jin, "Stable day-to-day dynamics for departure time choice," *Transportation Science*, vol. 54, no. 1, pp. 42–61, 2020.

[44] W.-L. Jin, "Stable local dynamics for day-to-day departure time choice," *Transportation Research Part B: Methodological*, vol. 149, pp. 463–479, 2021.

[45] J. Rouwendal, E. T. Verhoef, and J. Knockaert, "Verhoef and Jasper Knockaert. "Give or take? rewards versus charges for a congested bottleneck"," *Regional Science and Urban Economics*, vol. 42, no. 1-2, pp. 166–176, 2012.

[46] A. Kenneth, "Small. "The scheduling of consumer activities: work trips"," *The American Economic Review*, vol. 72, no. 3, pp. 467–479, 1982.